Mechanisms of imprint effect on ferroelectric thin films

Y. Zhou[a)]
Department of Applied Physics, The Hong Kong Polytechnic University, Hong Kong, China

H. K. Chan
School of Physics and Astronomy, The University of Manchester, Manchester M13 9PL, United Kingdom

C. H. Lam and F. G. Shin
Materials Research Centre and Centre for Smart Materials, The Hong Kong Polytechnic University, Hong Kong, China

(Received 17 September 2004; accepted 29 May 2005; published online 25 July 2005)

We have developed a single/double layer model to explain horizontal shifting of measured *D-E* hysteresis loops (imprint) for ferroelectric thin films. Such phenomenon can be explained by considering three mechanisms or their multiple effects: (1) stress induced by film/electrode lattice mismatch or clamping, (2) domain pinning induced by, e.g., oxygen vacancies, or (3) degradation of ferroelectric properties in film/electrode surface layers. First, it is found that hysteresis loops under the influence of stress exhibit large horizontal shifts with magnitudes comparable to those observed in experiments. Second, a pseudo-non-switching layer with a large coercive field is assumed to be present at the film/electrode interface in an otherwise homogeneous ferroelectric thin film, and in this case our simulation also shows a large imprint effect. Third, it is also found that time-dependent space-charge-limited conduction is likely to be one origin for the occurrence of imprint. © *2005 American Institute of Physics*. [DOI: 10.1063/1.1984075]

I. INTRODUCTION

Ferroelectric (FE) thin films have attracted much attention for the application of nonvolatile memories due to their bistable polarizations as well as small size. However, reliability problems such as fatigue and imprint have been obstacles for memory device application. It is therefore important to understand the physical mechanisms behind these failures in order to further advance ferroelectric materials into the memory market and provide a carefully directed improvement of these materials. Currently, three major failure mechanisms are believed to be limiting the lifetime of ferroelectric memory devices (FMD): fatigue, retention loss, and imprint. In this study, we aim to provide a better understanding of the physical origin of imprint, which is a horizontal shift of the *D-E* hysteresis loop measured from a Sawyer-Tower circuit. It is believed to be a result of the preference of one polarization state over another in ferroelectric bistability, which eventually leads to a failure when retrieving stored data.[1–5] Because of its influence in data storage, various efforts have been made to understand the origin of imprint.

Warren *et al.*[6] attributed the occurrence of imprint to defect dipoles related to oxygen vacancies. Abe and coworkers assumed a nonswitching layer between the ferroelectric layer and the bottom electrode, which is possibly formed by the relaxation of lattice misfit strain in the heteroepitaxial ferroelectric thin film.[5,7,8] Other explanations include domain pinning[1,2] and presence of surface layers.[4,5,9] However, all these mechanisms suggested have not been fully examined by accurate physical models or simulations, and there has not been a general agreement on a definitive mechanism for imprint. On the other hand, asymmetric polarization switching (different up- and down-switching processes) has also been investigated, for it is believed to be a likely origin of imprint. Wang *et al.*[10] phenomenologically modeled the asymmetric behavior of polarization switching by including an odd-power term in the expression of Landau's free energy. However, the physical origin of such asymmetry in polarization switching has not yet been identified. Hong *et al.* used a high-resolution atomic force microscopy (AFM) to investigate domain nucleation and growth during polarization switching in sol-gel-prepared lead zinconate titanate (PZT) thin films, and revealed that the forward domain growth is the rate-limiting mechanism.[11] Baudry used a lattice model to simulate the shifting of hysteresis loops and took into account the effects of nonuniform space charge by introducing a doping layer in the ferroelectric film near the electrode.[12] Lee *et al.* modeled shifted hysteresis loops by considering asymmetric electrode materials.[13] Lo and Chen demonstrated that effects of space charge and Schottky barrier heights in electrode materials could be the origin of the horizontal shifting of measured hysteresis loops.[14] Recently, Lü and Cao introduced asymmetric surface layers to represent the case of one easy polarization direction; the modeled asymmetry in the hysteresis loop is due to the presence of nonscreened depolarization field.[9] However, almost all the modeled hysteresis loops mentioned above did not shift as much as those observed in experiments.

We have developed a model in which the polarizations near the bottom electrode are much harder to reverse than the others under the applied alternating voltage, which leads to horizontal shifting of measured *D-E* loops. Warren *et al.* have already demonstrated that ionic defects, such as oxygen vacancies produced by reducing treatment, are responsible

[a)]Electronic mail: zhou.yan@polyu.edu.hk

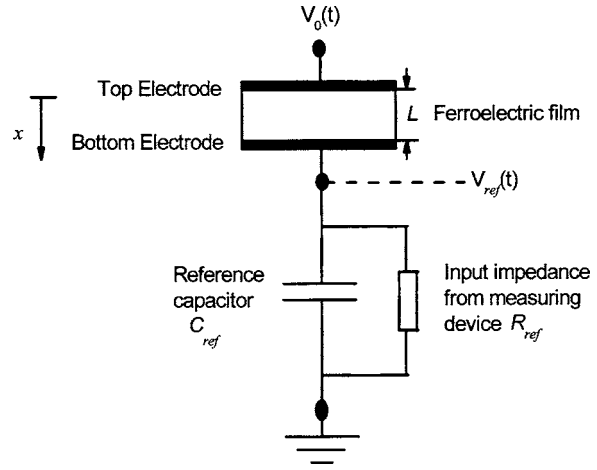

FIG. 1. Schematic diagram of the Sawyer-Tower circuit.

for ferroelectric domain pinning and formation of nonswitching layers, which shifts the hysteresis loops horizontally.[6] We propose that nonswitching layers may be formed by lattice misfit stress or by electronic charge trapping at domain boundaries, leading to the occurrence of imprint. By treating some layers near the bottom electrode as graded surface layers induced by some degradation mechanisms, our simulation successfully reproduced the large horizontal shifting of hysteresis loops observed in experiments. Our results demonstrate clearly that irreversible layers near the electrode induced by stress or by trapped defects are likely to be the origin of imprint failure. In general, our model shows a good agreement with experimental results in literature.

II. THEORETICAL CONSIDERATIONS AND NUMERICAL CALCULATION

A. Review of the Landau model for switching

A ferroelectric film, placed in a Sawyer-Tower circuit,[15] is modeled as a stacking of N thin layers; each layer has a thickness $\Delta x=L/N$, where L is the film thickness. We take $x=0$ at the interface between the ferroelectric film and the top electrode (Fig. 1) so that the position of any layer inside the film is given by $x=i\Delta x$, where $1\leqslant i\leqslant N$. The polarization and electric field at position x and time t are respectively denoted as $P(x,t)$ and $E(x,t)$ and are defined to be along the positive x direction. The total free energy of the film can be expressed by a Landau-type free-energy expression

$$F(t)=\sum_{i=1}^{N}\left\{\frac{\alpha(x)}{2}P(x,t)^2+\frac{\beta(x)}{4}P(x,t)^4+\frac{\kappa(x)}{2}\times[P(x,t)-P(x-\Delta x,t)]^2-P(x,t)E(x,t)\right\}, \quad (1)$$

where $\alpha(x)<0$ and $\beta(x)>0$ are the corresponding Landau coefficients at x. $\alpha(x)$ is temperature dependent: $\alpha(x)=a(x)\times(T-T_c)$, where $a(x)$ is a positive constant and the temperature T is smaller than the Curie temperature T_C. $\kappa(x)$ is the corresponding interaction coefficient between neighboring atoms. According to Landau's theory, the remanent polarization $P_r(x)$ and coercive field $E_c(x)$ are related to $\alpha(x)$ and $\beta(x)$ as

$$P_r(x)=\sqrt{-\frac{\alpha(x)}{\beta(x)}}, \quad (2)$$

$$E_c(x)=-\frac{2\alpha(x)}{3\sqrt{3}}\sqrt{-\frac{\alpha(x)}{\beta(x)}}. \quad (3)$$

The dynamics of dipoles is modeled using the Landau-Khalatnikov kinetic equation, which is a phenomenological equation of motion:

$$\frac{\partial P(x,t)}{\partial t}=-\frac{\partial F(t)}{\partial P(x,t)}=-\alpha(x)P(x,t)-\beta(x)P(x,t)^3+E(x,t)+\kappa(x)[P(x+\Delta x,t)+P(x-\Delta x,t)-2P(x,t)]. \quad (4)$$

The coefficient γ represents the viscosity that causes the delay in motion of individual dipole moments.

B. Time-dependent space-charge-limited conduction

In general, if there are inhomogeneities inside the ferroelectric film, the electric displacement $D(x,t)$ may not be spatially uniform. According to Gauss' law, there should be the presence of free space charges and the corresponding effect on electrical conduction has to be taken into account. In our previous study of compositionally graded ferroelectric film,[16] we derived the following formula for the time-dependent conductivity associated with space charges and named it time-dependent space-charge-limited (TDSCL) conduction:

$$\sigma(x,t)=\frac{\mu_p-\mu_n}{2}\frac{\partial D(x,t)}{\partial x}+\sqrt{\left[\frac{\mu_p+\mu_n}{2}\frac{\partial D(x,t)}{\partial x}\right]^2+\sigma_0(x)^2}. \quad (5)$$

$\sigma_0(x)$ is the intrinsic (Ohmic) conductivity; μ_p and μ_n are, respectively, the mobilities $(\mu_p,\mu_n>0)$ of p- and n-type free carriers, which we simply assume to be spatially invariant. Equation (5) was derived by borrowing the law of mass action from semiconductor physics;[16] we will here give a further justification to the application of this law for ferroelectric materials that are more or less insulators. We will also illustrate that Eq. (5) is reducible to the well-known Mott's equation for steady-state (time-independent) space-charge-limited conduction $(J\sim V^2)$, which is derived for linear dielectrics with a single-carrier type.[17] Equation (5) is therefore a more general formula for conduction involving space charges. For a detailed derivation of Eq. (5), please refer to Sec. II of Ref. 16.

The law of mass action in semiconductor physics states that the product of the concentrations of p- and n-type carriers is a constant. It is derived from (a) the equilibrium Fermi distribution of carriers in the absence of electric field, as well as from (b) the assumption that the distance of each band edge from the Fermi level is much larger than k_BT, where k_B is the Boltzmann constant and T is the temperature.[18] In the strictest sense, this law should not be applied in the presence

of an electric field because the carriers no longer obey the Fermi distribution function. In our case, the justifications for applying this law lie on the fact that (a) ferroelectric materials are essentially insulators and that (b) the frequency of the applied voltage is not very high (about 1 kHz). An insulator can be regarded as a wide-band-gap semiconductor and we may assume that the band gap is wide enough so that the distance of each band edge from the Fermi level is much larger than k_BT. Because it is an insulator, we may also assume that the system only undergoes a very small and negligible deviation from the equilibrium Fermi distribution. Furthermore, since the frequency of the applied voltage is not very high, any non-steady-state effect resulting from the time variation of electric field may be ignored.

To illustrate how Eq. (5) can be reduced to Mott's equation $J \sim V^2$, we recall that Eq. (5) was derived from the following definition of conductivity:[16]

$$\sigma(x,t) = q\mu_n[C_{\text{in}}(x) + \Delta n(x,t)] + q\mu_p[C_{\text{in}}(x) + \Delta p(x,t)], \tag{6}$$

with the intrinsic (Ohmic) conductivity given by

$$\sigma_0(x) = q[\mu_n + \mu_p]C_{\text{in}}(x). \tag{7}$$

For $\sigma_0(x) \to 0$ but $\sigma(x,t)$ being nonzero, we must have $C_{\text{in}}(x) \to 0$ and either μ_n or μ_p remaining finite. Since the carrier concentrations $[C_{\text{in}}(x) + \Delta n(x,t)]$ and $[C_{\text{in}}(x) + \Delta p(x,t)]$ are non-negative, for $C_{\text{in}}(x) \to 0$ we must have $\Delta n(x,t) \geqslant 0$ and $\Delta p(x,t) \geqslant 0$ and must be respectively equal to the n- and p-type carrier concentrations. Because $C_{\text{in}}(x) \to 0$, Eqs. (8) and (9) of Ref. 16 are reduced to

$$\Delta n(x,t)^2 + \Delta n(x,t)\left[\frac{1}{q}\frac{\partial D(x,t)}{\partial x}\right] \approx 0, \tag{8}$$

$$\Delta p(x,t)^2 + \Delta p(x,t)\left[-\frac{1}{q}\frac{\partial D(x,t)}{\partial x}\right] \approx 0, \tag{9}$$

so that

$$\Delta n(x,t) \approx 0 \text{ or } \Delta n(x,t) \approx -\frac{1}{q}\frac{\partial D(x,t)}{\partial x}, \tag{10}$$

$$\Delta p(x,t) \approx 0 \text{ or } \Delta p(x,t) \approx \frac{1}{q}\frac{\partial D(x,t)}{\partial x}. \tag{11}$$

The definition of space charge reads

$$\frac{\partial D(x,t)}{\partial x} = q[\Delta p(x,t) - \Delta n(x,t)]. \tag{12}$$

From Eqs. (10)–(12), it can be seen that only the following combinations of solutions are allowed:

$$\Delta n(x,t) \approx -\frac{1}{q}\frac{\partial D(x,t)}{\partial x} \text{ and } \Delta p(x,t) \approx 0, \tag{13}$$

$$\Delta p(x,t) \approx \frac{1}{q}\frac{\partial D(x,t)}{\partial x} \text{ and } \Delta n(x,t) \approx 0. \tag{14}$$

Thus, in the limit of zero intrinsic conductivity, we can only have the presence of the predominant carrier type. The p- and n-type carriers are mutually exclusive and they automatically reduce to a single-carrier condition. Since both $\Delta n(x,t)$ and $\Delta p(x,t)$ are non-negative, it can be seen from Eqs. (13) and (14) that $\partial D(x,t)/\partial x > 0$ necessarily implies the presence of only p-type carriers and $\partial D(x,t)/\partial x < 0$ the presence of only n-type carriers.

In the limit $\sigma_0(x) \to 0$, Eq. (5) becomes

$$\sigma(x,t) \approx \frac{\mu_p - \mu_n}{2}\frac{\partial D(x,t)}{\partial x} + \frac{\mu_p + \mu_n}{2}\left|\frac{\partial D(x,t)}{\partial x}\right|. \tag{15}$$

If $\partial D(x,t)/\partial x > 0$, it is

$$\sigma(x,t) \approx \frac{\mu_p - \mu_n}{2}\frac{\partial D(x,t)}{\partial x} + \frac{\mu_p + \mu_n}{2}\frac{\partial D(x,t)}{\partial x} = \mu_p\frac{\partial D(x,t)}{\partial x}. \tag{16}$$

And if $\partial D(x,t)/\partial x < 0$, it is

$$\sigma(x,t) \approx \frac{\mu_p - \mu_n}{2}\frac{\partial D(x,t)}{\partial x} - \frac{\mu_p + \mu_n}{2}\frac{\partial D(x,t)}{\partial x} = -\mu_n\frac{\partial D(x,t)}{\partial x}, \tag{17}$$

which are the original conditions from which Mott's result $J \sim V^2$ is derived, if we remove their time dependence.[17] It should be noted that, in the derivation of Eqs. (16) and (17), the mobility of the absent carrier type automatically disappears, and hence need not be deliberately suppressed. This puts our previous suggestion in Sec. II of Ref. 16 in a more general context.

C. Method of numerical simulation

In real hysteresis-loop measurements, the voltage $V_{\text{ref}}(t)$ of the reference capacitor is recorded against the average electric field $E_{\text{ave}}(t) = [V_0(t) - V_{\text{ref}}(t)]/L$ of the ferroelectric film (Fig. 1). The conservation of charge gives the continuity of the total current $J(t)$ across the circuit:

$$J(t) = \sigma(x,t)E(x,t) + \frac{\partial D(x,t)}{\partial t} = \frac{V_{\text{ref}}(t)}{R_{\text{ref}}A_{\text{ferro}}} + \frac{C_{\text{ref}}}{A_{\text{ferro}}}\frac{dV_{\text{ref}}(t)}{dt}, \tag{18}$$

with the electric displacement $D(x,t) = \varepsilon(x)E(x,t) + P(x,t)$ and the time-dependent conductivity given by Eq. (5). $\varepsilon(x)$ and A_{ferro} are, respectively, the dielectric permittivity and cross-sectional area of the ferroelectric film. C_{ref} and R_{ref} are, respectively, the capacitance and input impedance of the reference capacitor. The conservation of energy gives the vanishing of voltage sum across the circuit:

$$\int_0^L E(x,t)dx + V_{\text{ref}}(t) - V_0(t) = 0. \tag{19}$$

The initial conditions at time $t = 0$ are $P(x,0) = 0$, $E(x,0) = 0$, and correspondingly from Eq. (4), the derivative $[\partial P(x,t)/\partial t]_{t=0} = 0$ for all x inside the film. Having a sinusoidal applied voltage $V_0(t) = V_{0\,\max}\sin(\omega t)$ such that $V_0(0) = 0$, it follows from Eq. (19) that the initial voltage $V_{\text{ref}}(0)$ must also be zero. With all the above initial conditions speci-

TABLE I. The properties of the ferroelectric thin film and some related parameters used in our calculations.

Fig.	P_{rf} (μC cm^{-2})	E_{cf} (kV cm^{-1})	$\varepsilon_f/\varepsilon_0$	σ_{of} (10^{-11} Ω^{-1} m^{-1})	P_{rd} (μC cm^{-2})	E_{cd} (kV cm^{-1})	$\varepsilon_d/\varepsilon_0$	$V_{0\,max}$ (V)	ν
2	55	50	260	2.86	Nil	Nil	Nil	8.8	Nil
4	55	50	260	2.86	55	2000	260	20	0.1
5	55	50	260	2.86	55	2000	260	20	0.1
6	55	50	260	2.86	55	2000	260	13	Varied
8	55	50	260	2.86	Varied	50	Varied	20	0.1
9	55	50	260	2.86	Varied	50	Varied	20	Varied
10	55	50	260	2.86	Varied	50	Varied	20	0.1
11	55	50	260	2.86	Varied	50	Varied	20	0.1

fied, the values of every quantity at subsequent time steps can be computed by the forward Euler method.

The derivatives $\partial E(x,t)/\partial t$ and $dV_{ref}(t)/dt$ at time t can be determined from the following equations, which follows directly from Eqs. (18) and (19):

$$\frac{\partial E(x,t)}{\partial t} = \frac{\dfrac{V_{ref}(t)}{R_{ref}A_{ferro}} + \dfrac{C_{ref}}{A_{ferro}}\dfrac{dV_{ref}(t)}{dt} - J_c(x,t) - \dfrac{\partial P(x,t)}{\partial t}}{\varepsilon(x)}, \quad (20)$$

$$\frac{dV_{ref}(t)}{dt} = \frac{\dfrac{dV_0(t)}{dt} + \displaystyle\int_0^L \frac{J_c(x,t) + \dfrac{\partial P(x,t)}{\partial t}}{\varepsilon(x)}dx - \dfrac{\displaystyle\int_0^L \frac{1}{\varepsilon(x)}dx}{R_{ref}A_{ferro}}V_{ref}}{\dfrac{C_{ref}}{A_{ferro}}\displaystyle\int_0^L \frac{1}{\varepsilon(x)}dx + 1}, \quad (21)$$

so that the electric field and capacitor voltage at a later time $t+dt$ can be determined:

$$E(x,t+dt) = E(x,t) + \frac{\partial E(x,t)}{\partial t}dt, \quad (22)$$

$$V_{ref}(t+dt) = V_{ref}(t) + \frac{dV_{ref}(t)}{dt}dt. \quad (23)$$

By determining $\partial P(x,t)/\partial t$ from $E(x,t)$ and $P(x,t)$ using Eq. (4) (Landau-Khalatnikov), the polarization at $(t+dt)$ can also be determined:

$$P(x,t+dt) = P(x,t) + \frac{\partial P(x,t)}{\partial t}dt. \quad (24)$$

The foregoing formulation is employed in the investigation of the imprint effect discussed earlier. Except when especially defined, the values of the parameters which we use in the calculation are listed as follows:

$\mu_p = 0.25 \times 10^{-8}$ cm^2 V^{-1} s^{-1},

$\mu_n = 0.25 \times 10^{-5}$ cm^2 V^{-1} s^{-1}, $C_{ref} = 2.2 \times 10^{-8}$ F,

$A_{ferro} = 6.25 \times 10^{-8}$ m^2, $R_{ref} = 10^2$ MΩ,

$\kappa = 1$ kV cm/μC, $N = 200$, $dt = 10^{-9}$ s,

$\gamma = 1.0$ kV ms cm^4/μC, $f = \omega/2\pi = 1$ kHz,

$L = 800$ nm.

Also, except when especially emphasized, all the simulated loops shown in this paper have already reached their steady states.

III. RESULTS AND DISCUSSION

Stress, oxygen-vancancy-induced domain pinning, and film-electrode surface layers characterized by degradation of film properties have been suggested as possible origins of the imprint[1,2,4,5,7–9] and have therefore become the subject of our present investigation. Table I shows all the adopted values for the properties of the bulk and surface layers, as well as the applied field parameters, for our calculation in each figure.

A. Effect of stress

In heteroepitaxial films, the crystal structure may usually deviate from the original structure to a large extent.[7] As a result of clamping-induced electrode-film interaction[19,20] and the corresponding thermal or lattice mismatch[21] interfacial stress is always present at the surface. Müller and Thomas investigated the thickness dependence of early-stage stress development in two-dimensional solid film growth and obtained the following exponential stress distribution function: $\sigma'(x') = \sigma_0' e^{-x'/\alpha_t} = [\sigma_0' e^{-L/\alpha_t}]e^{x/\alpha_t}$, where $x' = L - x$ and σ_0' is the film/bottom electrode interfacial stress.[22] $\sigma_0' > 0$ and $\sigma_0' < 0$ represent the presence of tensile and compressive stress, respectively, and α_t is a parameter that describes the physics of long-range interactions between the deposited layers.

In the presence of stress, Eq. (1) should be expanded as

$$F = \sum_{i=1}^{N}\left[\frac{\alpha}{2}P_i^2 + \frac{\beta}{4}P_i^4 + \frac{\kappa}{2}(P_i - P_{i-1})^2 - P_iE_i + \frac{1}{2}Q\sigma_i'P_i^2 + \frac{1}{4}s\sigma_i'^2\right], \quad (25)$$

where Q is the electrostrictive coefficient and s is the elastic compliance constant. The Landau-Khalatnikov equation then becomes

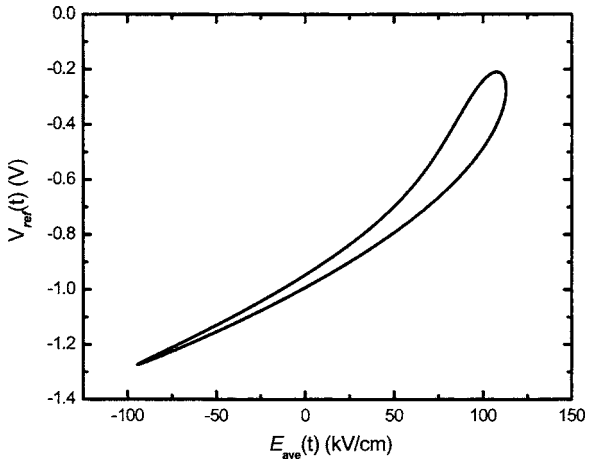

FIG. 2. Simulated *D-E* loop under the influence of compressive stress.

$$\gamma\frac{dP_i}{dt} = -\frac{\partial F}{\partial P_i} = -\alpha P_i - \beta P_i^3 + E_i + \kappa(P_{i+1} + P_{i-1} - 2P_i) - Q\sigma_i' P_i. \quad (26)$$

In our simulation, we use $\sigma_0' = -1.5\times10^9$ Pa and $Q = 6.6\times10^{-2}$ m^4/C^2. Figure 2 shows the simulated *D-E* loop by using the modeling approach discussed in Sec. II C, which is similar to the experimental loops reported in literature.[7,8,23–27] and therefore suggests that film-electrode lattice mismatch may be one possible origin of imprint.

Effects of stress on film properties have previously been investigated, where significant changes in hysteresis loop behavior have been observed.[28,29] Both experimental and theoretical results show that the coercive field E_c increases when the film is compressively stressed.[30,31] From the above-mentioned exponential stress distribution function, we know that the stress is maximum at the film/bottom electrode interface. The coercive field near the bottom electrode is thus likely to be larger than elsewhere so that the polarization in this region is much harder to reverse, inducing a pseudo-non-switching layer that is probably the ultimate origin of imprint.

B. Effect of domain pinning

Experimental results in literature show that domain pinning near film/electrode interfaces[32,33] is mainly caused by the presence of oxygen vacancies. Al-Shareef *et al.* proposed that electron trapping is a result of the alignment of defect-dipole complexes.[34] In particular, interface-trapped charges will lead to the pinning of dipoles which can be regarded as the preference of one polarization state over another. Such pinning phenomena have been reported for PZT and $BaTiO_3$ by Dimos and co-workers.[35,36] They showed that the occurrence of imprint can be attributed primarily to domain-wall pinning due to charge trapping.[36] He and Vanderbilt investigated the interaction between oxygen vacancies and domain walls using density-functional theory and then conducted a first-principles investigation of oxygen-vacancy pinning of domain walls in $PbTiO_3$.[37]

We assume that a pseudo-non-switching surface layer is formed at either film/electrode interface (Fig. 3). Compared

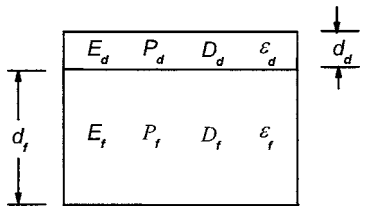

FIG. 3. Schematic diagram of a ferroelectric thin film consisting of two phases.

with the bulk, we assume that this surface layer has a much larger coercive field but roughly the same remanent polarization. In fact, it has been experimentally observed that the presence of defects or damage vacancies will induce a larger coercive field but a smaller remanent polarization,[38–42] making the polarization harder to reverse and producing a pseudo-domain-pinning effect in the surface layer. The electric displacements across the ferroelectric layer D_f and across the surface layer D_d are given by the following equations:

$$D_f = \varepsilon_f E_f + P_f, \quad (27)$$

$$D_d = \varepsilon_d E_d + P_d, \quad (28)$$

where E denotes electric field and P polarization, while the subscripts f and d denote the normal ferroelectric region and nonswitching surface layer, respectively. The average field across the thin film is calculated as

$$E_{\text{ave}} = (1-\nu)E_f + \nu E_d, \quad (29)$$

where ν represents the thickness fraction of the nonswitching layer in the film. Taking into account the surface nonswitching layer, the continuity of total current can be expressed as

$$J(t) = \sigma_f(x,t)E_f(x,t) + \varepsilon_f(x)\frac{\partial E_f(x,t)}{\partial t} + \frac{\partial P_f(x,t)}{\partial t}, \quad (30)$$

$$= \sigma_d(x,t)E_d(x,t) + \varepsilon_d(x)\frac{\partial E_d(x,t)}{\partial t} + \frac{\partial P_d(x,t)}{\partial t},$$

where $\sigma(x,t)$ and $\varepsilon(x)$ are the time-dependent space-charge-limited conductivity mentioned in Sec. II B and permittivity, respectively.

Figure 4(a) shows the simulated results of the *D-E* hysteresis loop for ferroelectric thin films in the presence of the pseudo-non-switching layer. The modeled *P-E* relations of the ferroelectric and nonswitching layers are respectively shown in Figs. 4(b) and 4(c). It can be seen that the hysteresis loop of the ferroelectric layer is completely cycled, while the polarization of the nonswitching layer only stays in the lower part of the *P-E* loop so that polarization switching cannot occur. The simulated *D-E* loop shown in Fig. 4(a) has a large horizontal shift to the right side, giving evidence that domain pinning within the surface layer could lead to an imprint. Loops with negative susceptibility like those depicted in Fig. 4(b) have already been reported in a paper describing the ferroelectric behavior of some barium titanate poled ceramics,[43] and Ricinschi *et al.* have discussed the physical meaning of the negative-susceptibility regions in hysteresis loops.[44] Figure 4 is obtained when we apply a

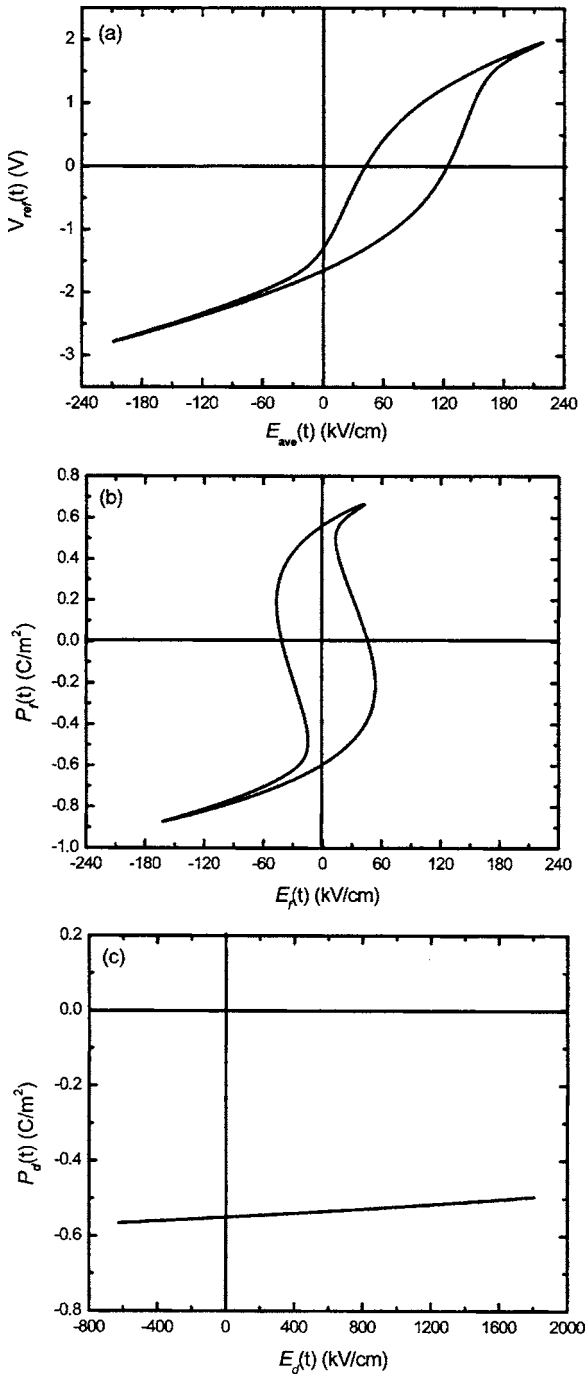

FIG. 4. When the polarization of the nonswitching layer only stays in the lower part of the *P-E* loop: (a) *D-E* hysteresis loop for ferroelectric thin films, (b) modeled *P-E* relations of the ferroelectric layer, (c) modeled *P-E* relations of the nonswitching layer.

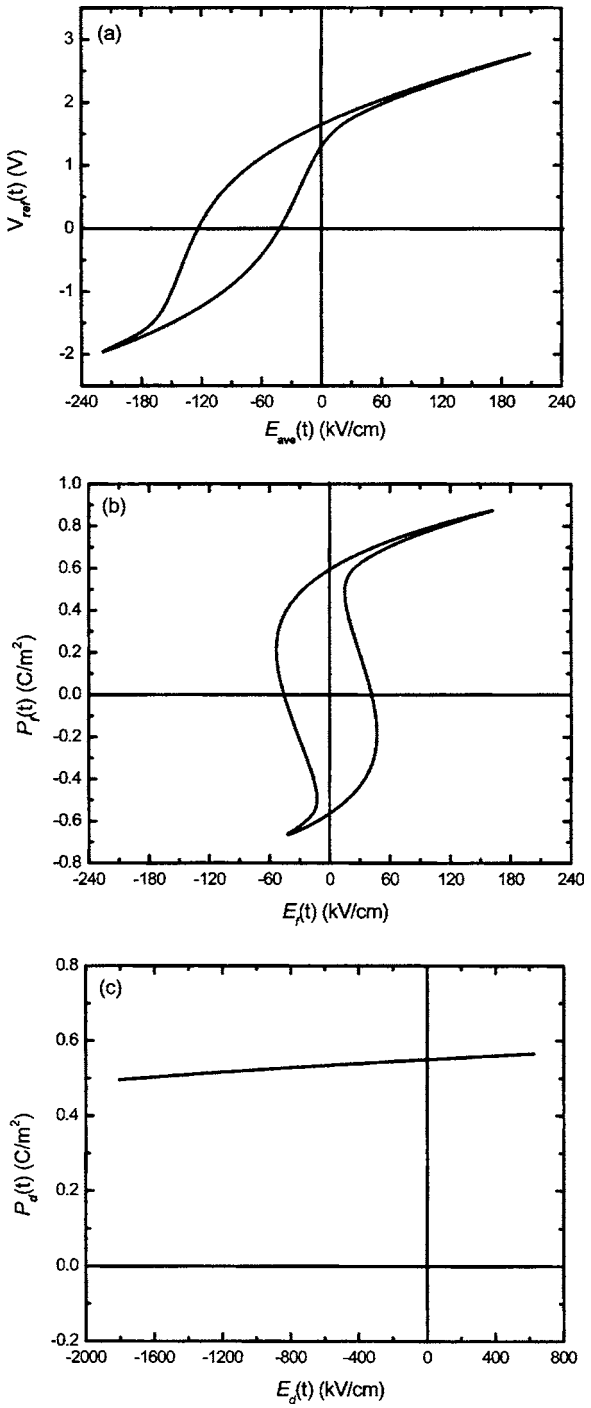

FIG. 5. When the polarization of the nonswitching layer only stays in the upper part of the *P-E* loop: (a) *D-E* hysteresis loop for ferroelectric thin films, (b) modeled *P-E* relations of the ferroelectric layer, (c) modeled *P-E* relations of the nonswitching layer.

sinusoidal wave without any initial phase. If there exists an initial phase π such that $V_0(t)=V_{0\,\max}\sin(\omega t+\pi)$, all the above-mentioned *D-E* and *P-E* relations only change by a 180° flip about the x and y axis, as shown in Fig. 5. It is because in the nonswitching layer the polarization stays in the upper part of the loop instead of in the lower part, as shown in Fig. 5(c). It should be noted that the types of "long-tail" hysteresis loops shown in Fig. 4(a) and Fig. 5(a) exhibit a striking similarity with those observed in experiments,[3,7,8,25,27] thus justifying the validity of our model that includes a pseudo-non-switching surface layer. Figure 6 shows the effect of the thickness ratio of the nonswitching layer on the hysteresis loop. When $\nu=0.01$, the simulated loop almost centers at the origin and no notable horizontal shift is observed. With ν increasing, the magnitude of the horizontal shift increases. Therefore, our model should be confined to the study of thin ferroelectric films where the surface layer has an appreciable thickness fraction.

We have used a double-layer model with an abrupt interface to model the imprint effect under the influence of domain pinning near the film/electrode interface. Similar re-

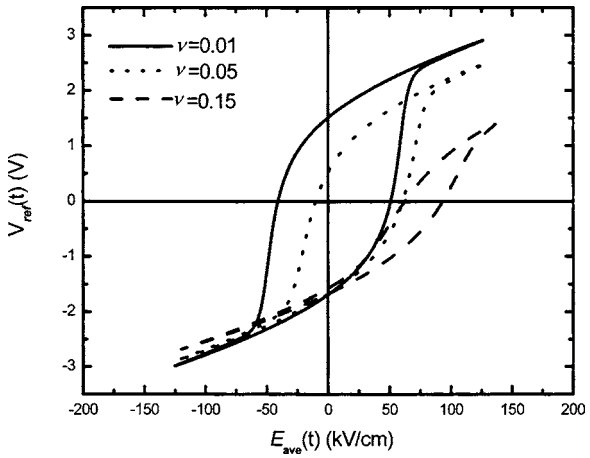

FIG. 6. Effect of the thickness ratio of the nonswitching layer on the hysteresis loop.

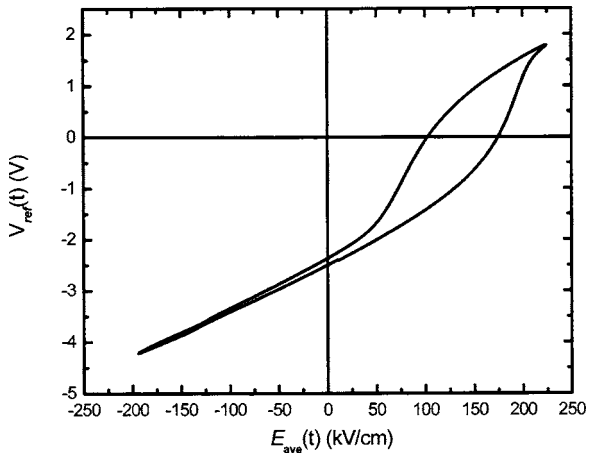

FIG. 8. Measured *D-E* loop simulated from our model with a graded surface layer near the bottom electrode.

sults are obtained if the interface is replaced by a smoother one with gradual variation in properties. We have also calculated the shift effect by assuming Ohmic conductivity alone, i.e., assuming $\sigma(x,t) \approx \sigma_0$ and not using the full TDSCL conductivity expression in Eq. (5). It is found that a shift also exists and that the shift magnitudes are about one third to one half of the shift magnitudes from the TDSCL conduction calculations for some typical σ_0 values of a ferroelectric thin film.[16] We therefore suggest that the TDSCL conduction is likely one of the dominating factors even in the presence of domain pinning for the occurrence of large imprint effects observed in experiments.

C. Effect of graded surface layer

It has been known experimentally that ferroelectric properties of surface layers such as remanent polarization and permittivity are weaker than those of the bulk region.[45–47] Such degradation of ferroelectric properties[19] has been suggested to occur for reasons such as: (a) interdiffusion between a ferroelectric thin film and electrode,[48] (b) insufficient flatness of bottom electrode and film, and (c) vacancies of Pb and/or oxygen.[49] It is justifiable to model the surface layer as a graded one in which the permittivity and remanent polarization decrease gradually from the bulk values (Fig. 7). Figure 8 shows the measured *D-E* loop simulated from our model incorporating a graded surface layer near the bottom electrode, for which a large horizontal shift is produced (see Table II for related parameters). Note that this type of hysteresis loop can be found in related experimental measurements.[6] Figure 9 shows the effect of the thickness ratio of the graded layer on the hysteresis loop; the magnitude of the horizontal shift increases with the fraction of the graded layer. Figure 10(a) illustrates two cases where only the Ohmic conductivity is considered and where the effect of the TDSCL conduction is taken into account. There is almost no horizontal shift when only the Ohmic conductivity is considered, but a notable horizontal shift is observed when the TDSCL conduction is taken into account. Figure 10(b) shows the time evolution of interfacial charge $(=D_d - D_f)$ for, respectively, the consideration and the neglect of the TDSCL conduction. It is interesting to see that there is an average positive interfacial charge accumulated when the TDSCL conduction is taken into account, while there is almost no interfacial charge accumulation for the case when only the Ohmic conduction is considered. Figure 11 shows the time development of electric fields in the bulk ferroelectric layer (E_f) and the graded surface layer (E_d); a large positive dc bias has accumulated in the graded surface layer while a much smaller negative dc bias has done so in the bulk layer. On the other hand, the electric-field distributions inside the bulk and graded surface layers are both nonuniform. The electric field tends to be concentrated within the graded surface layer, possibly because this region tends to acquire a strong field for polarization reversal.[7] It is found that the measured *D-E* loop shifts to the opposite side when the

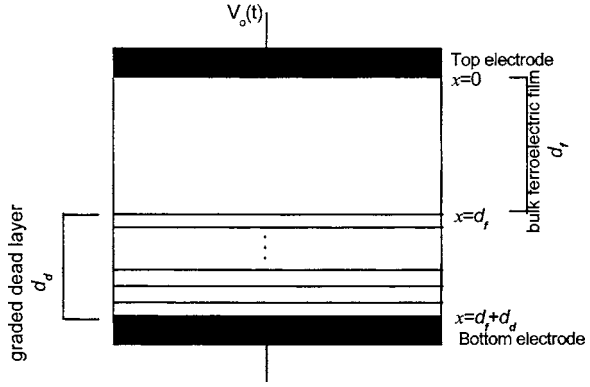

FIG. 7. Ferroelectric thin film consisting of bulk ferroelectric and graded surface layers whose thicknesses are respectively d_f and d_d.

TABLE II. The variations of remanent polarization and permittivity of the graded surface layer with x.

$(x-d_f)/d_d$	$P_{rd}(x)$ (μC cm^{-2})	$\varepsilon_d(x)/\varepsilon_0$
0	55	260
0.25	26.4	210
0.5	11.8	160
0.75	5.4	110
1	1.2	60

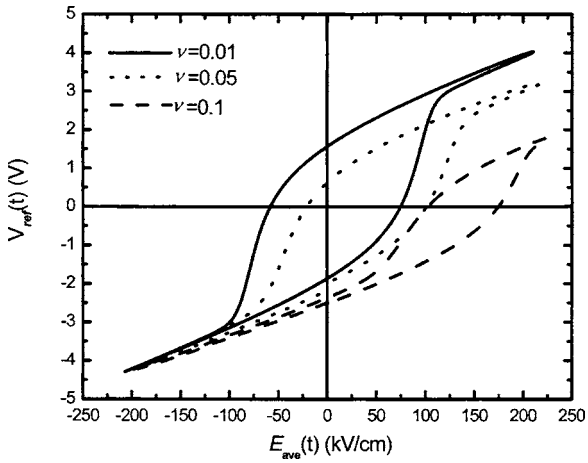

FIG. 9. Effect of the thickness ratio of the graded layer on the hysteresis loop.

graded surface layer is placed adjacent to the top electrode instead of the bottom one, where the gradient of the surface layer is reversed; i.e., the direction of horizontal shift is determined by the gradient of the surface layer.

Summing up, we have taken the TDSCL conduction into account to investigate the effects of stress, domain pinning, and graded surface layer on the hysteresis loops. In the first and third cases, the consideration of the TDSCL conduction is necessary to lead to the horizontally shifted hysteresis loops; while the Ohmic conduction is also able to give a horizontal shift behavior when considering domain pinning, it is unable to produce large shift magnitudes observed in some ferroelectric thin film systems. Therefore, although the consideration of the TDSCL conduction is not a requisite for the shift effect in all cases, it is likely to be one of the possible origins for the occurrence of imprint where large shifts of hysteresis loops are observed in experiments.

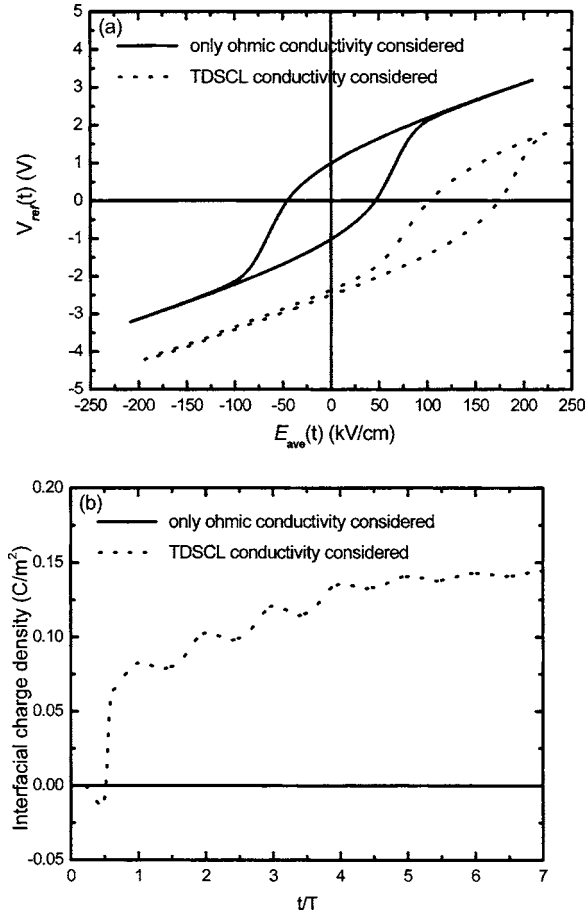

FIG. 10. Effects of TDSCL and Ohmic conductivities: (a) on the simulated *D-E* loop and (b) on the time evolution of interfacial charge densities.

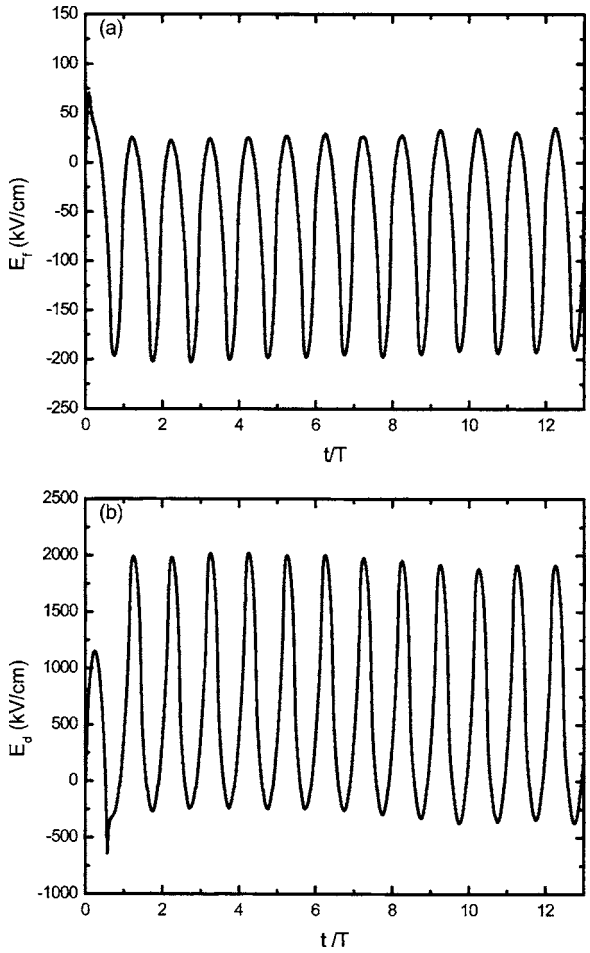

FIG. 11. Time development of electric fields: (a) in the bulk ferroelectric layer and (b) in the graded surface layer.

In general, the qualitative similarity between published experimental results and our simulation shows that stress, domain pinning induced by, e.g., oxygen vacancies, and graded surface layers or their multiple effects are likely to be responsible for the widely observed imprint phenomena. Our model can be extended to study how different parameters like thickness, permittivity, and spontaneous polarization of the bulk and surface layers affect hysteresis loop measurement.

IV. CONCLUSIONS

A model has been introduced to explain the occurence of imprint phenomena widely reported in literature. This model adopts the Landau-Khalatnikov equation to describe the hysteresis behavior and takes the time-dependent space-charge-limited conductivity into account to investigate the effects of stress, domain pinning, and degradation of ferroelectric prop-

erties at film/electrode surface. Our calculation produces the large horizontally shifted loops by considering the effects of stress and nonswitching layers. The qualitative agreement between simulation and experiment supports the notion that imprint phenomena may originate from stress induced by lattice mismatch or clamping effect of the substrate, domain pinning induced by defect-dipole alignments, and/or the existence of graded surface layer. However, further efforts are needed to better understand the physics behind the imprint effect.

ACKNOWLEDGMENT

The authors acknowledge the support of an internal grant from Hong Kong Polytechnic University.

[1]D. Nagasawa and H. Nozawa, Jpn. J. Appl. Phys., Part 1 **38**, 5406 (1999).
[2]W. Liu, J. Ko, and W. Zhu, Mater. Lett. **49**, 122 (2001).
[3]S. Aggarwal and R. Ramesh, Annu. Rev. Mater. Sci. **28**, 463 (1998).
[4]M. Joseph, A. M. Randall, and F. B. McLean, *Proc. 3rd Int. Symp. Integr. Ferroelectr.*, edited by R. Panhozler (Gordon & Breach, Switzerland, 1991), pp. 44–70.
[5]K. Abe, N. Yanase, T. Yasumoto, and T. Kawakubo, Jpn. J. Appl. Phys., Part 1 **41**, 6065 (2002).
[6]W. L. Warren, B. A. Tuttle, D. Dimos, G. E. Pike, H. N. Al-Shareef, R. Ramesh, and J. T. Evans, Jpn. J. Appl. Phys., Part 1 **35**, 1521 (1996).
[7]K. Abe, S. Komatsu, N. Yanase, K. Sano, and T. Kawakubo, Jpn. J. Appl. Phys., Part 1 **36**, 5846 (1997).
[8]K. Abe and S. Komatsu, J. Appl. Phys. **77**, 6461 (1995).
[9]T. Lü and W. Cao, Microelectron. Eng. **66**, 818 (2003).
[10]C. L. Wang, L. Zhang, Y. P. Peng, W. L. Zhong, P. L. Zhang, and Y. X. Wang, Solid State Commun. **109**, 213 (1999).
[11]S. Hong, E. L. Colla, E. Kim, D. V. Taylor, A. K. Tagantsev, P. Muralt, K. No, and N. Setter, J. Appl. Phys. **86**, 607 (1999).
[12]L. Baudry, J. Appl. Phys. **86**, 1096 (1999).
[13]K. W. Lee, Y. I. Kim, and W. J. Lee, Ferroelectrics **271**, 1769 (2002).
[14]V. C. Lo and Z. J. Chen, IEEE Trans. Ultrason. Ferroelectr. Freq. Control **49**, 980 (2002).
[15]C. B. Sawyer and C. H. Tower, Phys. Rev. **35**, 269 (1930).
[16]H. K. Chan, C. H. Lam, and F. G. Shin, J. Appl. Phys. **95**, 2665 (2004).
[17]R. Coelho, *Physics of Dielectrics for the Engineer* (Elsevier Science, New York, 1979), pp. 123–125.
[18]J. R. Hook and H. E. Hall, *Solid State Physics* (Wiley, Chichester, New York 1974), pp. 139–143.
[19]Y. Saya, S. Watanabe, M. Kawai, H. Yamada, and K. Matsushige, Jpn. J. Appl. Phys., Part 1 **39**, 3799 (2000).
[20]Y. Li, V. Nagarajan, S. Aggarwal, R. Ramesh, L. G. Salamanca-Riba, and L. J. Martinez-Miranda, J. Appl. Phys. **92**, 6762 (2000).
[21]M. Grossmann, O. Lohse, D. Bolten, U. Boettger, and R. Waser, J. Appl. Phys. **92**, 2688 (2002).
[22]P. Müller and O. Thomas, Surf. Sci. **465**, 764 (2000).
[23]B. H. Park, T. W. Noh, J. Lee, C. Y. Kim, and W. Jo, Appl. Phys. Lett. **70**, 1101 (1997).
[24]S. K. Dey, J. J. Lee, and P. Alluri, Jpn. J. Appl. Phys., Part 1 **34**, 3142 (1995).
[25]B. H. Park, S. J. Hyun, C. R. Moon, B. D. Choe, J. Lee, C. Y. Kim, W. Jo, and T. W. Noh, J. Appl. Phys. **84**, 4428 (1998).
[26]Y. H. Xu, C. J. Chen, and R. Xu, J. Appl. Phys. **67**, 2985 (1990).
[27]W. B. Wu, K. H. Wong, and C. L. Mak, J. Vac. Sci. Technol. A **18**, 2412 (2000).
[28]S. B. Desu, J. Electrochem. Soc. **140**, 2981 (1993).
[29]T. Kumazawa, Y. Kumagai, H. Miura, and M. Kitano, Appl. Phys. Lett. **72**, 608 (1998).
[30]G. A. C. M. Spierings, G. J. M. Dormans, W. G. J. Moors, M. J. E. Ulenaers, and P. K. Larsen, J. Appl. Phys. **78**, 1926 (1995).
[31]T. K. Song, J. S. Kim, M. H. Kim, W. Lim, Y. S. Kim, and J. Lee, Thin Solid Films **424**, 84 (2003).
[32]W. B. Wu, K. H. Wong, G. K. H. Pang, and C. L. Choy, Appl. Phys. Lett. **86**, 072904 (2005).
[33]G. E. Pike, W. L. Warren, D. Dimos, B. A. Tuttle, R. Ramesh, J. Lee, V. G. Keramidas, and J. T. Evans, Appl. Phys. Lett. **66**, 484 (1995).
[34]H. N. Al-Shareef, D. Dimos, W. L. Warren, and B. A. Tuttle, Integr. Ferroelectr. **15**, 53 (1997).
[35]S. Sadashivan, S. Aggarwal, T. K. Song, R. Ramesh, J. T. Evans, B. A. Tuttle, W. L. Warren, and D. Dimos, J. Appl. Phys. **83**, 2165 (1998).
[36]D. Dimos, H. N. Al-Shareef, W. L. Warren, and B. A. Tuttle, J. Appl. Phys. **80**, 682 (1996).
[37]L. X. He and D. Vanderbilt, Phys. Rev. B **68**, 134103 (2003).
[38]I. Stoilichnov, A. Tagantsev, E. Colla, S. Gentil, S. Hiboux, J. Baborowski, P. Muralt, and N. Setter, J. Appl. Phys. **88**, 2154 (2000).
[39]C. L. Li, Z. H. Chen, Y. L. Zhou, and D. F. Cui, J. Phys.: Condens. Matter **13**, 5261 (2001).
[40]M. Shimizu, M. Okaniwa, H. Fujisawa, and H. Niu, Jpn. J. Appl. Phys., Part 1 **41**, 6686 (2002).
[41]U. Robels, J. H. Calderwood, and G. Arlt, J. Appl. Phys. **77**, 4002 (1995).
[42]R. Loloee and M. A. Crimp, J. Appl. Phys. **92**, 4541 (2002).
[43]H. G. Baerwald and D. A. Berlincourt, J. Acoust. Soc. Am. **25**, 703 (1953).
[44]D. Ricinschi, C. Harnagea, C. Papusoi, L. Mitoseriu, V. Tura, and M. Okuyama, J. Phys.: Condens. Matter **10**, 477 (1998).
[45]Y. Sakashita, H. Segawa, K. Tominaga, and M. Okada, J. Appl. Phys. **73**, 7857 (1993).
[46]T. Hase, T. Sakuma, Y. Miyasaka, K. Hirata, and N. Hosokawa, Jpn. J. Appl. Phys., Part 1 **32**, 4061 (1993).
[47]A. K. Tagantsev, M. Landivar, E. Colla, and N. Setter, J. Appl. Phys. **78**, 2623 (1995).
[48]T. Nakamura, Y. Nakao, A. Kamisawa, and H. Takasu, Jpn. J. Appl. Phys., Part 1 **33**, 5207 (1994).
[49]J. Lee, A. Safari, and R. L. Pfeffer, Appl. Phys. Lett. **61**, 1643 (1992).